Modeling and Simulation of the Photocatalytic Treatment of Wastewater using Natural Bauxite and TiO₂ doped by Quantum Dots

Nidhal Becheikh[1†], Aboulbaba Eladeb[1], Nejib Ghazouani[1]

Northern Border University (NBU), College of Engineering, Arar, Saudi Arabia.

Summary

The photocatalytic degradation of salicylic acid takes place in several stages involving coupled phenomena, such as the transport of molecules and the chemical reaction. The systems of transport equations and the photocatalytic reaction are numerically solved using COMSOL Mutiphysics (CM) simulation software. CM will make it possible to couple the phenomena of flow, the transport of pollutants (salicylic acid) by convection and diffusion, and the chemical reaction to the catalytic area (bauxite or TiO2 doped by nanoparticles). The simulation of the conversion rate allows to correctly fit the experimental results. The temporal simulation shows that the reaction reaches equilibrium after a transitional stage lasting over one minute. The outcomes of the study highlight the importance of diffusion in the boundary layer and the usefulness of injecting micro-agitation into the microchannel flow. Under such conditions, salicylic acid degrades completely.

Keywords:
Modeling, Simulation, Photocatalytic reaction, Microreactor, Micro-agitation.

1. Introduction

As a measure to eliminate persistent pollution, advanced treatments must be applied, including the destruction of residual pollutants with advanced oxidation (AOTs) such as photocatalysis and ozonation. Advanced oxidation processes (AOPs) rely on the production of highly reactive oxidative species, mainly OH° hydroxyl radicals. This radical has several advantages over other oxidants, in particular thanks to its non-selectivity. The photocatalysis is among the most efficient oxidation techniques. However, industry-grade photocatalytic requires further research for better control and sizing of its seat reactors. The micro-structuring of reactors is an novel approach that was taken to solve the problem. Indeed, the use of microfluidic systems will improve the mass transfer between the gas-liquid and liquid-catalyst phases. An experimental study

and modeling of the kinetics of photocatalytic degradation of an organic pollutant are established in this work. Among the most used catalyst in photocatalysis is TiO₂ [1-3]. When this catalyst is exposed to UV radiation, the photons are absorbed and an electron migrates to the conduction band leaving a hole in the valence band [2-6]. The use of photocatalysts is today accompanied by doping by luminescent nanoparticles (QDs). They make it possible to minimize the electron-hole recombination phenomena and to improve the catalyst performance. The development of the synthesis of nanoparticles and their use to improve the performances of the catalysts is in full expansion [7]. It allows, once mastered, a rapid production at large-scale [7, 8]. Nanomaterials are distinguished by a large specific surface area (surface/volume ratio), which improves the adsorption of pollutants on this surface as well as their subsequent degradation. Both bauxite and titanium dioxide (TiO₂) are widely used as semi-conductor photocatalysts [9-17]. They are commonly used for water depollution by advanced oxidation routes [17-20]. Most of nanoparticle properties are directly related to the particle size and the shape. The diffusion of light and therefore, the visibility of the particles are consequently minimized [21]. On the other hand, the small size of the nanoparticles allows them to reach the most confined places [22-26]. Finally, the most commonly used method for carrying out this photocatalytic degradation reaction is the fixed bed microreactor, which offers a specific surface and a long residence time [27].

2. Materials and Methods

2.1. Experimental procedure

The experimental procedure first concerns the preparation of ZnO-based nanoparticles by mixing zinc acetate and NaOH as a sol gel route. The nanoparticles are then separated from the solvent through centrifugation at 3000 rpm for five minutes, filtered, and lastly precipitated. The purification step is done by washing the nanoparticles with acetone solution and then distilled water to eliminate residues. The retained nanoparticles are vacuum dried at 40°C for 12 hrs. Finally, the TiO2 catalyst will be doped with ZnO-based nanoparticles. Pure bauxite is used and examined during testing. Using a Thermo Scientific Evolution 300 UV–Visible spectrophotometer, the absorbance of the solutions and their concentration at various time intervals were measured. The conversion rate is given by Eq. 1:

$$X = \left(\frac{C_0 - C_t}{C_0}\right) \tag{1}$$

Where C_0 and C_t are respectively, the initial and exit concentrations of salicylic acid.

2.2. Modeling and simulation

2.2.1 Modeling of photocatalytic reaction

The conservation equations are determined from the global and partial balances of the microreactors:

     - The flow in the microreactors is independent of the gravity forces,

     - The flow regime is laminar,

     - The fluid is Newtonian and incompressible.

Taking these assumptions into account, the mass conservation is written as follows (Eq.2):

$$\nabla.(\rho \vec{U}) = 0 \tag{2}$$

Where ρ is the density (kg/m³) and U the flow velocity vector (m/s).

The Navier-Stokes equations (Eq. 3) describe the principle of momentum conservation, taking into account the flow laws of fluid mechanics:

$$\nabla.(\rho \vec{U} \otimes \vec{U}) = -\nabla p + \nabla.\mu(\nabla \vec{U} + \nabla \vec{U}^T) \tag{3}$$

The evolution of the concentration in the presence of a chemical reaction is written as shown by Eq. 4:

$$\nabla.(\vec{U}C) = -\nabla.\vec{J} + r \tag{4}$$

With r representing the rate of the reaction and C the concentration of salicylic acid. The rate of photocatalytic degradation on a catalytic surface is given, using the Langmuir-Hinshelwood model, by:

$$r = k_r \frac{KC_S}{1 + KC_S} \tag{5}$$

Where k_r is the apparent rate constant of reaction, K is the adsorption constant and C_s the concentration of salicylic acid at the catalytic surface. When the reaction is faster than the transport to the catalytic surface, a concentration gradient develops between the reaction medium of concentration Cm and the catalytic surface of concentration Cs. The flow of matter, proportional to the concentration gradient, is given by Fick's law:

$$\vec{J} = -D_m \nabla C \tag{6}$$

With D_m presenting the molecular diffusion coefficient of salicylic acid.

2.2.2 Simulation of photocatalytic reaction

A. Microreactor geometry

The selected geometric model is a parallel plane microreactor with a reactive surface corresponding to the bottom of the microchannel (Figure 1). Despite the microchannel's two-dimensional representation, the numerical simulation will account for the microchannel's width (3rd dimension).
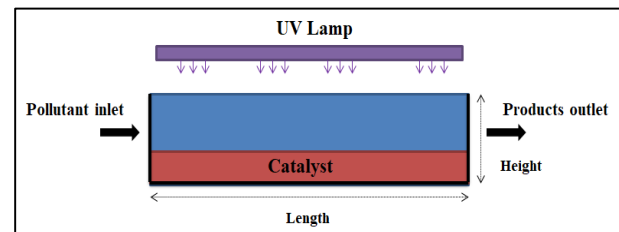

Figure1: Schematic representation of the reaction domain.

B. Meshing

The COMSOL Mutiphysics computer code can use square, triangular and other types of more complex meshes. It is common practice to apply a non-regular mesh to the entire studied system. The mesh may be tightened close to points of interest. The mesh can be tightened close to target area the catalytic surface (Figure 2).
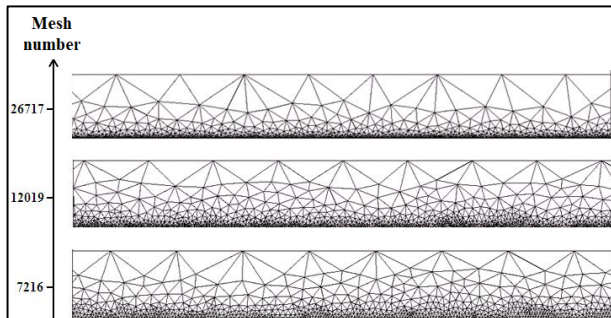

Figure 2: 2D domain meshing.

The computation time and the precision of the results are very sensitive to the quality of the mesh. The number of meshes that can be chosen is limited by how much free memory the device has and how long it takes to do the calculations..

C. Convergence criterion

The residuals are calculated for concentration, velocity, and pressure to evaluate the degree of imbalance in the equation corresponding to each variable. The convergence criterion is met when the residual value is sufficiently small. In our case, the surface concentration residual must approach 10^{-6} in order for the result to remain unchanged.

3. Results of photocatalytic degradation simulation

At the start of the experiment, when the UV lamp was off, the concentration of the pollutant dropped before reaching an adsorption-desorption equilibrium and caused a concentration gradient to appear in the reaction medium. At the beginning (t=0), we can assume that the initial concentration far from the catalytic surface is uniform (C_m=10 mg/L=0.072 mol/m^3) and that the initial concentration at the catalytic surface is zero.
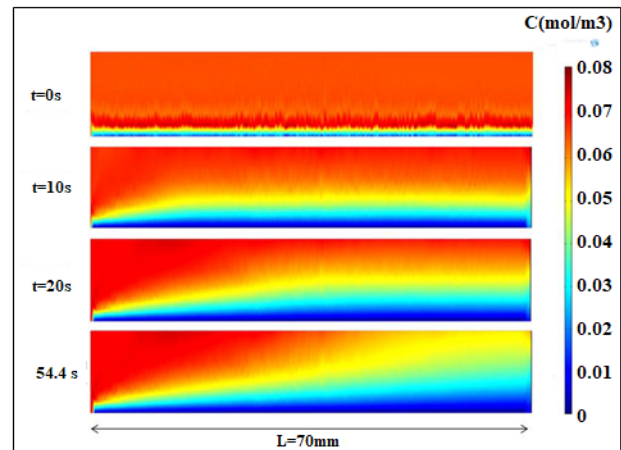

Figure 3: Concentration gradients in the microreactor as a function of time, for Q=2.5 mL/h and C_0=10 mg/L using TiO$_2$-ZnO (NP).

The thickness of the diffusion boundary layer (Figure 3) is of the same order of magnitude as the height of the microchannel. For a flow rate of 2.5 mL/h, the thickness of the diffusion boundary layer is large enough to consider that the diffusive flux is not negligible. The concentration gradient gradually increases in the microreactor as a function of time. At the exit of the microchannel, the average concentration decreases gradually to reach a final conversion rate (Figure 4).
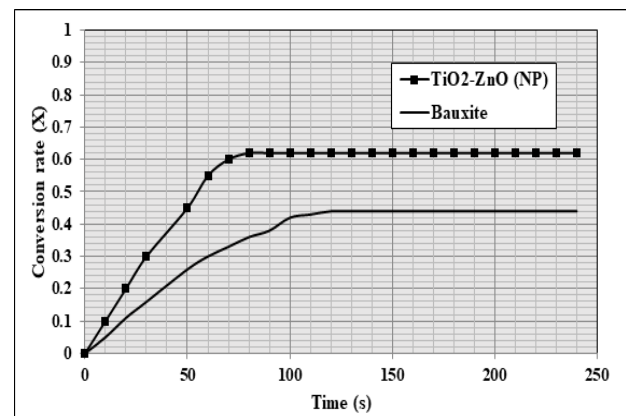

Figure 4: Temporal conversion rate r using TiO$_2$-ZnO (NP) and bauxite catalyst.

The simulation of the conversion rate as a function of the flow rate was carried out with a kinetic constant k_r and an

adsorption constant K. These constants allow a good correlation of the experimental results (Figure 5). The conversion rate increases very rapidly in the presence of irradiation and reaches a level corresponding to the adsorption-desorption equilibrium.
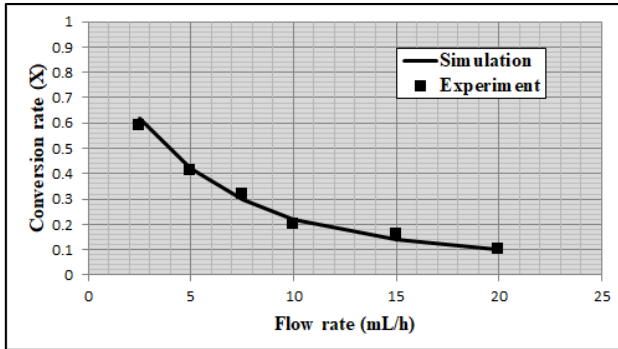

Figure 5: Conversion rate as a function of the flow rate in the microreactor TiO_2-ZnO (NP).

To increase the probability a molecule located at a height greater than the thickness of the diffusion boundary layer collides with the catalytic surface, we simulated the photocatalytic degradation in the microreactor by adding a known number of 0.25 mm-long baffles, i.e, half the depth of the microchannel. These baffles impose a radial flow of the fluid towards the catalytic surface. The influence of baffles number is shown in Figure 6.
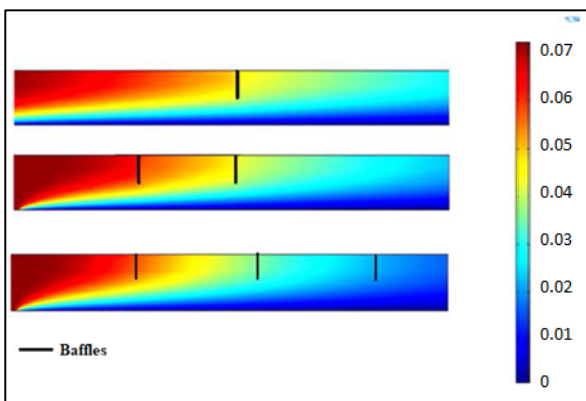

Figure 6: Concentration gradients as a function of baffles number.

Comparing numerical estimations with respect to the baffles layouts in the micro-channel, the highest conversion

rate is recorded for the micro-channel with three baffles (Figure 7). In this instance, the salicylic acid is completely degraded at a flow rate of 2.5 mL/h. At high flow rates, the influence of the baffles regardless their number is even more pronounced compared to reference micro-channel (without baffle).
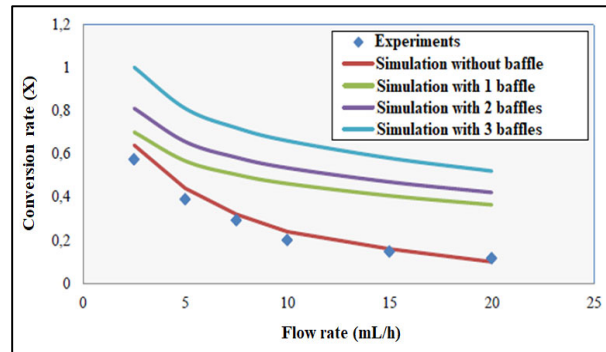

Figure 7: Conversion rate as function of flow rate for different baffle configurations using TiO_2-ZnO(NP).

Velocity gradient profiles were determined via numerical simulation performed for different baffle configurations. The flow velocity in the microreactor increases considerably in the vicinity of the baffles for a flow rate of 2.5 mL/h. As a result of the vortex effect caused by the baffle, the flow rate stays the same at Q=2.5mL/h, but the flow speed increases by a lot close to the vortex Far away from the singularity zone, the velocity distribution is again uniform in the flow direction(Figure 8).
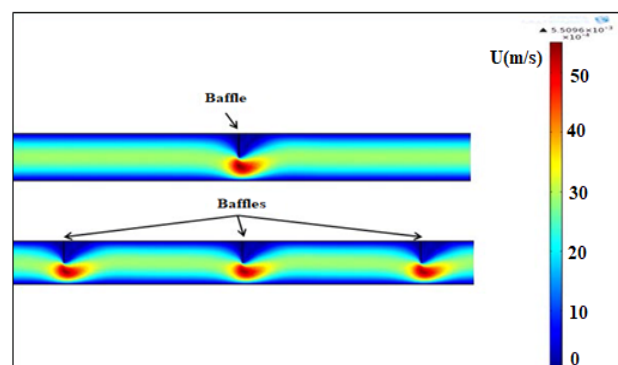

Figure 8: Flow velocity gradients in the microchannel for one-baffle and three-baffle layouts.

4. Conclusion

The photocatalytic degradation of salicylic acid takes place in several steps involving coupled phenomena including the transport of molecules and the chemical reaction. The systems of transport equations and the photocatalytic reaction are solved numerically using COMSOL Mutiphysics (CM). The simulation model developed in CM has enabled the coupling of flow phenomena, pollutant transport (salicylic acid) via convection and diffusion, and the chemical reaction to the catalytic zone (bauxite or TiO2 doped with nanoparticles).. The simulated conversion rates are used to adjust the experimental results. The temporal simulation also shows that the steady state of the reaction is reached after a reaction transitory stage longer than one minute. The results demonstrate the essential role of boundary layer diffusion and the importance of introducing micro flow agitation in the microchannel. Indeed, in this case, salicylic acid can be completely degraded.

At the beginning of the experiment, when the UV lamp is switched off, the concentration of the pollutant drops before reaching an adsorption-desorption equilibrium and causes a concentration gradient to appear in the reaction medium. The thickness of the diffusion boundary layer is of the same order as the height of the microchannel. For a flow rate of 2.5 mL/h, the thickness of the diffusion boundary layer is sufficiently great to consider that the diffusive flux is not negligible. To increase the probability of encounter between a molecule located at a height greater than the thickness of the diffusion boundary layer and the catalytic surface, we simulated the photocatalytic degradation in the microreactor by adding a known number of baffles of 0.25 mm length. These baffles impose a radial flow of the fluid towards the catalytic surface. By adding three baffles inside the micro-channel with uniform longitudinal configuration, it has been shown that three-baffle configuration is interesting with respect to the conversion rates. As illustration, results all the salicylic acid is degraded for a flow rate of 2.5 mL/h. For higher flow rates, the conversion rates are less sensitive to the number of baffles present placed inside the microchannel. However, with comparison to reference configuration (a microchannel without baffle), the conversion rates are more pronounced.

References
[1] Jeon, S., & Braun, P. V. Hydrothermal synthesis of Er-doped luminescent TiO2 nanoparticles. Chemistry of Materials, 15(6), 1256-1263 (2003).
[2] Bera, D., et al., Photoluminescence of ZnO quantum dots produced by a sol–gel process. Optical Materials. 30(8): p. 1233-1239(2008).
[3] Carrasco-Jaim, O.A., et al., Photocatalytic hydrogen production by biomimetic indium sulfide using Mimosa pudica leaves as template. international journal of hydrogen energy, 44(5): p. 2770-2783 (2019).
[4] Chen, C., et al., Preparation and photocatalytic performance of graphene Oxide/WO3 quantum Dots/TiO2@ SiO2 microspheres. Vacuum, 164: p. 66-71 (2019). .
[5] Chen, W.-T., et al., Performance comparison of Ni/TiO2 and Au/TiO2 photocatalysts for H2 production in different alcohol-water mixtures. Journal of catalysis,367: p. 27-42 (2018). .
[6] Chen, Y., H. Ding, and S. Sun, Preparation and characterization of ZnO nanoparticles supported on amorphous SiO2. Nanomaterials. 7(8): p. 217. (2017).
[7] Chen, Z., et al., A sol–gel method for preparing ZnO quantum dots with strong blue emission. Journal of Luminescence. 131(10): p. 2072-2077. (2017).
[8] Danish, R., F. Ahmed, and B.H. Koo, Rapid synthesis of high surface area anatase titanium oxide quantum dots. Ceramics International. 40(8): p. 12675-12680. (2014).
[9] Desa, A.L., et al., A comparative study of ZnO-PVP and ZnO-PEG nanoparticles activity in membrane photocatalytic reactor (MPR) for industrial dye wastewater treatment under different membranes. Journal of Environmental Chemical Engineering, 7(3): p. 103143. (2019).
[10] Diab, K.R., et al., Facile fabrication of NiTiO3/graphene nanocomposites for photocatalytic hydrogen generation. Journal of Photochemistry and Photobiology A: Chemistry,. 365: p. 86-93. (2018).
[11] Dosado, A.G., et al., Novel Au/TiO2 photocatalysts for hydrogen production in alcohol–water mixtures based on hydrogen titanate nanotube precursors. Journal of catalysis,. 330: p. 238-254. (2015).

[12] Deng, Bona, et al. "Photocatalytic activity of CaTiO3 derived from roasting process of bauxite residue." Journal of Cleaner Production 244 ,118598. (2020).

[13] Ismail, N. J., Othman, M. H. D., Bakar, S. A., Kadir, S. H. S. A., Abd Aziz, M. H., Pauzan, M. A. B., ... & Rahman, M. A. Hydrothermal synthesis of TiO2 nanoflower deposited on bauxite hollow fibre membrane for boosting photocatalysis of bisphenol A. Journal of Water Process Engineering, 37, 101504. (2020).

[14] Nurul Jannah, "Hydrothermal synthesis of TiO2 nanoflower deposited on bauxite hollow fibre membrane for boosting photocatalysis of bisphenol A." Journal of Water Process Engineering 37 101504. (2020).

[15] Ismail, Nurul Jannah, et al. "Characterization of Bauxite as a Potential Natural Photocatalyst for Photodegradation of Textile Dye." Arabian Journal for Science and Engineering 44.12 10031- 10040. (2019).

[16] Lu, Qing-hua, Yue-hua Hu, and Meng Wang. "Photocatalytic activity of bauxite-tailings supported nano-TiO 2." Journal of Central South University of Technology 17.4 ,755-759. (2010).

[17] Guevara, Hero Paul R., et al. "Recovery of oxalate from bauxite wastewater using fluidized-bed homogeneous granulation process." Journal of Cleaner Production 154 130-138. (2017).

[18] El-Maghrabi, H.H., et al., Synthesis of mesoporous core-shell CdS@ TiO2 (0D and 1D) photocatalysts for solar-driven hydrogen fuel production. Journal of Photochemistry and Photobiology A: Chemistry, 351: p. 261-270. (2017).

[19] Fakhroueian, Z., et al., Influence of modified ZnO quantum dots and nanostructures as new antibacterials. Advances in nanoparticles. 2(03): p. 247. (2013).

[20] Gao, G., et al., Selectivity of quantum dot sensitized ZnO nanotube arrays for improved photocatalytic activity. Phys Chem Chem Phys, 19(18): p. 11366-11372. (2017).

[21] Gnanasekaran, L., R. Hemamalini, and K. Ravichandran, Synthesis and characterization of TiO2 quantum dots for photocatalytic application. Journal of Saudi Chemical Society. 19(5): p. 589-594. (2015).

[22] Gruzintsev, A., et al., Luminescence of two-dimensional ordered array of the ZnO quantum nanodots, obtained by means of the synthetic opal. Thin solid films. 459(1-2): p. 111-114. (2014).

[23] Guo, Z., et al., Synthesis of 3D CQDs/urchin-like and yolk-shell TiO2 hierarchical structure with enhanced photocatalytic properties. Ceramics International. 45(5): p. 5858-5865. (2019).

[24] Iqbal, M., et al., Photocatalytic degradation of organic pollutant with nanosized cadmium sulfide. Materials Science for Energy Technologies. 2(1): p. 41-45. (2019).

[25] Javed, S., M. Islam, and M. Mujahid, Synthesis and characterization of TiO2 quantum dots by sol gel reflux condensation method. Ceramics International. 45(2): p. 2676-2679. 10. (2019).

[26] Khan, R., et al., Low-temperature synthesis of ZnO quantum dots for photocatalytic degradation of methyl orange dye under UV irradiation. Ceramics international. 40(9): p. 14827-14831. (2014).

[27] Kumaravel, V., et al., Photocatalytic hydrogen production using metal doped TiO2: A review of recent advances. Applied Catalysis B: Environmental, (2019).

[28] Zubair, M., et al., Solar spectrum photocatalytic conversion of CO2 to CH4 utilizing TiO2 nanotube arrays embedded with graphene quantum dots. Journal of CO2 Utilization. 26: p. 70-79. (2018).

Nidhal Becheikh earned the BSc degree, from the National School of Engineering, Gabes University in 2007. He received the MSc degree in 2009 from Lyon University and he received the Dr. Eng. degree from Lorraine Universityin 2012. Currently, he is an assistant professor in the department of Chemical and Materials Engineering at Northern Border University since 2017. His research interests include mass and heat transfer processes, and optimization of chemical engineering equipment.

Aboulbaba Eladeb received the BSc. degree, from National School of Engineering, Gabes University, in 2008. He earned the MSc and thePhD degrees from Lorraine University in 2009 and 2014, respectively. He has been an assistant professor in the department . of Chemical and Materials Engineering at Northern Border University since 2015. Renewable energy and chemical engineering processes for separation are among his research interests.

Nejib Ghazouani earned the BSc. MSc and PhD degrees, from Tunis El Manar university in 2003, 2007, and 2012, respectively. After working as an assistant professor in Tunis University, heis currently, is an assistant professor in the department of Civil Engineering at Northern Border University since 2014. His research interest includes continuum mechanics, and structure theories along with environmental engineering.